Influence of Conducting Polymers Based on Carboxylated Polyaniline on *In Vitro* $CaCO_3$ Crystallization

Andrónico Neira-Carrillo,*[,†] Diego F. Acevedo,[‡] Maria C. Miras,[‡] Cesar A. Barbero,[‡] Denis Gebauer,[§] Helmut Cölfen,*[,§] and José L. Arias[†]

Faculty of Veterinary and Animal Sciences, University of Chile and Center for Advanced Interdisciplinary Research in Materials (CIMAT), Santiago, Chile, Faculty of Exact Sciences, Universidad Nacional de Río Cuarto, Córdoba, Argentina, and Max-Planck-Institute of Colloids and Interfaces, Colloid Chemistry, Research Campus Golm, D-14424 Potsdam, Germany

Conducting polymers are interesting materials of technological applications, while the use of polymers as additives controlling crystal nucleation and growth is a fast growing research field. In the present article, we make a first step in combining both topics and report the effect of conducting polymer derivatives, which are based on carboxylated polyanilines (c-PANIs), on *in vitro* $CaCO_3$ crystallization by the Kitano and gas diffusion method. This is the first example of the mineralization control of $CaCO_3$ by a rigid carboxylated polymer. Both the concentration of c-PANI and the presence of carboxylate groups have a strong influence on the $CaCO_3$ crystallization behavior and crystal morphology. X-ray diffraction (XRD) analysis shows crystalline calcite particles confirmed by FTIR spectra. pH and Ca^{2+} measurements during $CaCO_3$ crystallization utilizing the Kitano and a constant-pH approach show a defined nucleation period of $CaCO_3$ particles. The measurements allow for the calculation of the supersaturation time development, and the kinetic data can be combined with time-dependent light microscopy. The presence of c-PANIs delays the time of nucleation indicative of calcite nucleation inhibition. Microscopy illustrates the morphologies of $CaCO_3$ crystals at all crystallization stages, from homogeneous spherical amorphous $CaCO_3$ (ACC) particles corresponding to the first steps of crystallization to transition stage calcite crystals also involving a dissolution−recrystallization process in a late stage of crystallization. The data show that it is not possible to conclude the crystallization mechanism even for a very simple additive controlled crystallization process without time-resolved microscopic data supplemented by the analysis of the species present in the solution. Finally, fluorescence analysis indicates that conducting polymer derivatives can be incorporated into precipitated calcite particles. This gives rise to $CaCO_3$ particles with novel and interesting optical properties.

1. Introduction

Biological crystallization (biomineralization) is a widespread phenomenon in nature, in which minute amounts of organic components exert substantial control over inorganic mineralization. Mineralization control results in the formation of particles of uniform size, novel and complex crystal morphologies, specific crystallographic orientation, hierarchical order, and interesting properties.[1] *In vivo*, biominerals are synthesized at ambient conditions in an aqueous environment and are fully biodegradable. *In vitro* synthesis of inorganic materials of specific size, architecture, and morphology at the microscale and nanoscale levels is a key aspect in fields as diverse as modern materials, medicine, electronics, ceramics, pigments, and cosmetics.[2] Here, calcium carbonate ($CaCO_3$) is one of the most studied systems which can facilitate the understanding of biological control of mineralization.[3,4] For instance, the synthesis and control of amorphous $CaCO_3$ nanoparticles with regular morphology is a crucial challenge of increasing importance due to their strong influence on materials properties and future applications.[5] The majority of $CaCO_3$ crystallization studies addressing biological control over mineralization have been done by applying an organic substrate (additive). It is well-known that the crystallization mechanism is altered by specific interactions with chemical groups such as $-CO_2H$, $-PO_3H$, and $-SO_3H$.[6−9] Polyelectrolytes (among them, water-soluble block copolymers with a polyelectrolyte block) turned out to be extraordinarily effective crystal growth modifiers.[10−13] The resulting morphology of synthetic crystals is often an expression of different growth rates in the various crystallographic directions. From a thermodynamic point of view, the obtained crystal morphology minimizes the free enthalpy of the crystal which is the sum of the products of surface energy and area of all exposed faces (Wulff's rule).[14] This has the consequence that low energy surfaces become exposed and high energy surfaces vanish. Crystal surface energies can be lowered by the adsorption of additives present in solution, and the crystal morphology alters correspondingly.[15] According to

* To whom correspondence should be addressed. Telephone: +56-2-9785642 (A.N.-C.); +49-0-331567 9513 (H.C.). Fax: +56-2-9785526 (A.N.-C.); +49-0-3315679502 (H.C.). E-mail: aneira@uchile.cl (A.N.-C.); coelfen@mpikg-golm.mpg.de (H.C.).

† University of Chile and Center for Advanced Interdisciplinary Research in Materials (CIMAT).

‡ Universidad Nacional de Río Cuarto.

§ Max-Planck-Institute of Colloids and Interfaces.

(1) Lowenstam, H. A.; Weiner, S. *On Biomineralization*; Oxford University Press: Oxford, 1989; Chapter 3.

(2) Mann, S.; Ozin, G. A. *Nature* **1996**, *382*, 313–318.

(3) Meldrum, F. C. *Int. Mater. Rev.* **2003**, *48*, 187–224.

(4) Cölfen, H. *Curr. Opin. Colloid Interface Sci.* **2003**, *8*, 23–31.

(5) Pai, R. K.; Pillai, S. *CrystEngComm* **2008**, *10*, 865–872.

(6) Grassmann, O.; Löbmann, P. *Biomaterials* **2004**, *25*, 277–282.

(7) Arias, J. L.; Neira-Carrillo, A.; Arias, J. I.; Escobar, C.; Bodero, M.; David, M.; Fernandez, M. S. *J. Mater. Chem.* **2004**, *14*, 2154–2160.

(8) Mann, S.; Archibald, D. D.; Didymus, J. M.; Douglas, T.; Heywood, B. R.; Meldrum, F. C.; Reeves, N. J. *Science* **1993**, *261*, 1286–1292.

(9) Mann, S.; Archibald, D. D.; Didymus, J. M.; Heywood, B. R.; Meldrum, F. C.; Wade, V. J. *MRS Bull.* **1992**, 32–36.

(10) Yu, S. H.; Cölfen, H. J. *Mater. Chem.* **2004**, *14*, 2124–2147.

(11) Cölfen, H. *Macromol. Rapid Commun.* **2001**, *22*, 219–252.

(12) Pai, R. K.; Pillai, S. *Cryst. Growth Des.* **2007**, *7*, 215–217.

(13) Xu, A. W.; Ma, Y. R.; Cölfen, H. J. *Mater. Chem.* **2007**, *17*, 415–449.

(14) Wulff, G. *Z. Kristallogr.* **1901**, *34*, 449–530.

Wulff's rule, planes on which the additives are adsorbed become generally expressed as crystals faces.[16]

On the other hand, polyaniline (PANI), in which the polymer backbone structure is conjugated (alternating single and double bonds), is one of the most studied conjugated conducting polymers due to its interesting properties such as environmental stability, good electrical conductivity, low cost, and easy chemical and electrochemical synthesis.[17] The usual way to produce functionalized conductive polymers involves the synthesis or acquisition of an already functionalized monomer and its homopolymerization or copolymerization. An alternative way involves postpolymerization functionalization of a well-known conducting polymer. Some typical conducting polymers are polyacetylene, polyaniline, and polypyrrole.[18] Although classical applications are related to electrical and conducting coating fields, nowadays it is possible to create new conducting polymer transistors with switching speeds based on charge state changes similar to neurons. This can be applied in biomimetic systems such as actuators (muscles), computation (neurons), information transmission (nerves), structural elements (bones), energy absorption and storage, and so forth.[19] A limitation of PANI in such applications is its low solubility in common solvents and poor miscibility with other polymers. However, it is possible to synthesize derivatives of PANI exhibiting improved properties by the inclusion of functional groups such as carboxylic and sulfonic groups in a simple way using covalent bonding of reactive molecules bearing functional groups into the polymer backbone.[20,21] The functionalization process makes this kind of polymers versatile materials and good candidates for controlling the course of $CaCO_3$ crystallization. These functionalized PANI polymers are especially interesting as additives for $CaCO_3$ crystallization, since they are rigid polymers,$^{-36}$ so that the carboxylated derivative is the first example of a rigid carboxylated polymer additive for $CaCO_3$ crystallization control. The use of conducting PANI polymers as additives for $CaCO_3$ crystallization (or other inorganic materials such as zinc oxide or hydroxyapatite) is yet unknown and opens a new field of research in order to find new applications of them and synthesis strategies for hybrid materials, for example, for electrically conducting or fluorescent $CaCO_3$ films.[22] Coating with derivatives of PANI polymers by specific interactions with individual growth planes of $CaCO_3$ crystals could retain electrical properties, such as color, conductivity, fluorescence, corrosion resistance, and so forth. Recently, Aizenberg and Han[23] reported calcite crystal recrystallization on a $Au-C_{15}-CO_2H$ template from the amorphous calcium carbonate (ACC) phase. The crystals retained fluorescence when fluorescent dyes were chosen as dopants. Furthermore, incorporation of photoluminescence properties into layered lanthanide silicate nanoparticles, which are suitable for the engineering of functional materials for ink-jet printing, sensors, or energy transfer, has been reported.[24] Enhanced fluorescence, for instance, induced by Au-colloid self-assembled monolayers of two different fluorophore−protein conjugates on a solid glass support has also been achieved.[25] The authors report strong variations of fluorescence enhancement by both interparticle distance and particle size. Basically, small particles quench fluorescence, because adsorption dominates over scattering, an effect clearly apparent in the optical extinction spectra.[26] Thus, it is possible to improve the enhancement of the fluorescence lifetime properties by the systematic control of particle size and interparticle distance.[25,26] In that respect, incorporation of PANI derivatives into $CaCO_3$ crystal matrices might improve important properties of paper applications and coatings (e.g., color and brightness, dimensional stability, and density), in which $CaCO_3$ crystals could be used as filler materials. In fact, similar applications using calcite crystals and hollow spherical $CaCO_3$ as fillers in papermaking have been proposed in order to improve optical and brightness properties and inhibit the opacity of the resulting paper.[27] We report the effect of conducting PANI derivatives, which are based on carboxylated polyanilines (c-PANIs), on the crystal growth of $CaCO_3$ using gas diffusion[28] and Kitano solution methods[29−31] as slow crystallization methods in order to test for a possible PANI inclusion into the crystal lattice as is already reported for biominerals,[32] crystallization inhibition effects, as well as the morphogenesis of $CaCO_3$.

2. Materials and Methods

2.1. Materials. All reagents and solvents were of the highest available grade. Distilled water was obtained from a capsule filter 0.2 μm flow (U.S. Filter), and bidistilled water was used for preparing all solutions and Kitano solution. $CaCO_3$ powder (99+%) from Sigma-Aldrich, calcium chloride dihydrate, ethanol, and tris(hydroxymethyl) aminomethane from ACS-Merck, and ammonium hydrogen carbonate (NH_4HCO_3) from J.T. Baker were used without further purification.

2.2. Methods. Scanning electron microscopy (SEM) measurements of $CaCO_3$ from gas diffusion crystallization were done with a TESLA BS 343A scanning electron microscope at 15 kV. Gold coating (20 nm thick) was done with an EMS-550 automated sputter coater. Energy dispersive X-ray spectroscopy (EDX) was performed using a JEOL JSM-5410 scanning electron microscope (SEM-EDX) at 15 kV. In the case of Kitano crystallization, both light microscopy (LM) in solution and SEM were applied to all samples. The use of LM was necessary to prove that the SEM micrographs show real structures instead of drying artifacts resulting from the sample preparation. The SEM measurements were performed on a DSM940A instrument (Carl Zeiss, Jena), and the pictures were taken with a digital camera connected to the scanning electron microscope. The $CaCO_3$ crystals were directly taken from the solution. LM images were taken in solution at the same time with an Olympus BX 41 microscope and a VHX digital microscope (Keyence VH-Z500). Fourier transform infrared spectra (FTIR) were obtained on a FTS 6000 spectrometer (Bio-Rad Laboratories, Inc.). Wide-angle X-ray diffraction data (WAXS) were taken from a powdered sample using an ENRAF Nonius FR 590 diffractometer with Cu Kα radiation.

(15) Didymus, J. M.; Oliver, P.; Mann, S.; DeVries, A. L.; Hauschka, P. V.; Westbroek, P. *J. Chem. Soc., Faraday Trans.* **1993**, *89*, 2891–2900.
(16) Weissbuch, L.; Addadi, M.; Lahav, L.; Leiserowitz, L. *Science* **1991**, *253*, 637–645.
(17) Acevedo, D. F.; Salavagione, H. J.; Miras, M. C.; Barbero, C. A. *J. Braz. Chem. Soc.* **2005**, *16*, 259–269.
(18) Carraher, C. E. *Seymour/Carraher's Polymer Chemistry*, 4th ed.; Marcel Dekker: New York, 1996.
(19) Madden, P. G.; Madden, J. D.; Anquetil, P. A.; Yu, H.-h.; Swager, T. M.; Hunter, I. W. Bio-Robotics Symposium, The University of New Hampshire, Durham, NH, Aug 27−29, 2001.
(20) Yue, J.; Wang, Z. H.; Cromack, K. R.; Epstein, A. J.; MacDiarmid, A. G. *J. Am. Chem. Soc.* **1991**, *113*, 2665–2671.
(21) Heeger, A. J. *Angew. Chem., Int. Ed.* **2001**, *40*, 2591–2611.
(22) Sindhu, S.; Jegadesan, S.; Li, H.; Ajikumar, P. K.; Vetrichelvan, M.; Valiyaveettil, S. *Adv. Funct. Mater.* **2007**, *17*, 1698–1704.
(23) Aizenberg, J.; Han, T. Y.-J. *Chem. Mater.* **2008**, *20*, 1065–1068.
(24) Ananias, D.; Ferdov, S.; Almeida Paz, F. A.; Sá Ferreira, R. A.; Ferreira, A.; Geraldes, C. F. G. C.; Carlos, L. D.; Lin, Z.; Rocha, J. *Chem. Mater.* **2008**, *20*, 205–212.
(25) Xie, F.; Baker, M. S.; Goldys, E. M. *Chem. Mater.* **2008**, *20*, 1788–1797.
(26) Lakowicz, J. R. *Anal. Biochem.* **2005**, *337*, 171–194.
(27) Hadiko, G.; Han, Y. S.; Fuji, M.; Takahashi, M. *Mater. Lett.* **2005**, *59*, 2519–2522.
(28) Domínguez-Vera, J. M.; Gautron, J.; García-Ruiz, J. M.; Nys, Y. *Poult. Sci.* **2000**, *79*, 901–907.
(29) Kitano, Y.; Park, K.; Hood, D. W. J. *Geophys. Res.* **1962**, *67*, 4873–4874.
(30) Dimova, R.; Lipowsky, R.; Mastai, Y.; Antonietti, M. *Langmuir* **2003**, *19*, 6097–6103.
(31) Rudloff, J.; Cölfen, H. *Langmuir* **2004**, *20*, 991–996.
(32) Addadi, L.; Weiner, S. *Proc. Natl. Acad. Sci. U.S.A.* **1985**, *82*, 4110–4114.

Table 1. Molecular Weight and Solubility of PANI and c-PANIs at pH 10

sample	MW (g/mol)	solubility ($\times 10^{-3}$ g/cm^{-3})
c-PANI	82 000	0
c-PANI-1	34 000	3.2($\pm$0.1)
c-PANI-2	26 000	4.2($\pm$0.1)
c-PANI-3	98 000	8.3($\pm$0.1)

Transmission electron microscopy (TEM) and electron diffraction were performed on an EM 912 Ω (Zeiss) instrument.

2.3. Polymer Syntheses. *2.3.1. Copolymers.* Poly(aniline-*co*-3-aminobenzoic acid) (c-PANI-1)[33] was synthesized by chemical oxidation in an acidic medium (HCl, 1 M) following a common procedure for PANI synthesis.[34] The copolymerization was done in an ice bath (0 °C), as described before,[35] with vigorous stirring, and the copolymer was washed with 1 M HCl (soluble oligomers were eliminated) and water. The product was dried under vacuum for 24 h. Poly(aniline-*co*-2-aminoterephthalic acid) (c-PANI-2) was synthesized, as described before,[36] by chemical oxidation with ammonium persulphate in equimolar ratio with the monomer in acidic medium (1 M HCl). The copolymerization was done in an ice bath (0 °C) with vigorous stirring during at least 3 h, and the copolymer was washed with 1 M HCl and water. c-PANI-3 was obtained by modification of PANI with the diazonium salt of 4-aminobenzoic acid.[17]

2.3.2. Functionalized Polymer (c-PANI-3). Polyaniline (emeraldine form) was prepared by oxidation of aniline (0.1 M) in 1 M HCl with ammonium persulphate (equimolar) at temperatures below 5 °C. The temperature was monitored during the polymerization. When the reaction was completed, after the maximum temperature was reached, the polymer was filtered out under suction and washed with 1 M HCl solution (500 mL) and water (1 L). The polymer was then converted into its base form by stirring for 24 h in a 0.1 M NH_4OH solution. The diazonium salt of the aromatic amine, *p*-aminobenzoic acid (PABA), was made by reaction of PABA with sodium nitrite (equimolar to the amine) and concentrated HCl in an ice bath.[17] The PANI powder was then suspended in TRIS buffer (pH = 8) and mixed with the diazonium salt of PABA in an ice bath. After 30 min, the solid was filtered out using vacuum and washed first with 1 L of 1 M HCl solution and then with 1 L distilled water. The solid was then dried under vacuum for 48 h. All copolymer compositions of c-PANIs were measured through elemental analysis using the C/N ratio. The copolymer composition is obtained assuming that aniline homopolymers ($F = 1$), that is, $F_{ANI} = x/(x + y)$, are defined as the molar fraction of aniline units in the copolymer and assuming that PANI has a C/N ratio equal to 6 and the corresponding C/N ratio values of the homopolymer acids (e.g., c-PANI-1 with C/N ratio equal to 7). Therefore, the values (F_{ANI}) were expressed as mole fractions, c-PANI-1 (0.87), c-PANI-2 (0.70), and c-PANI-3 (0.38). The c-PANI polymers had different molecular weights ranging from 26 000 to 98 000 g/mol, depending on the composition. Particularly, c-PANI-1, c-PANI-2, and c-PANI-3 had molecular weights of 34 000, 26 000, and 98 000 g/mol, respectively. The molecular weights of c-PANIs were determined using static light scattering in *N*-methylpyrrolidone (NMP) with dimethylformamide (DMF). The molecular weight of PANI was 82 000 g/mol determined in NMP with LiCl (Table 1). On the other hand, it is well-known that the low solubility of PANI could be increased using functional groups attached to the backbone. Therefore, all the used c-PANI polymers are more soluble than the PANI polymer in common solvents (acetone, toluene, $CHCl_3$, and NH_3/*i*PrOH). The modified polymer is soluble in common solvents and for our experimental conditions at pH 9.00, unlike PANI which is only soluble in concentrated acids and NMP. Table 1 shows a comparison of the solubility of PANI with c-PANI polymers and the MWs.

The study of the solubility of c-PANIs in pH 10 solution was performed as follows. The doped form of each copolymer in powder was ground up with a mortar before solubility testing. A total of 0.01 g of the polymer was added to 10 mL of solvent and stirred for 1 h before filtering. The filter paper was preweighed, and then the filtrate was allowed to evaporate and dry under vacuum during 24 h before weighing the papers again to calculate the solubility of c-PANIs. In all cases, the c-PANI solubilities are higher than the concentrations used here.

2.4. Crystallization Methods. The crystallization of $CaCO_3$ was based on the gas diffusion and Kitano solution methods. The gas diffusion crystallization was performed for 24 h, and the pH was fixed using TRIS buffer. In the case of the Kitano method, the kinetic parameters, which are the determining factor of morphogenesis in the gas diffusion method, allow us to study the effect of the c-PANIs in a slow crystallization process, in which the kinetic effect disappears showing highly reproducible kinetics with a slow nucleation. The gas diffusion method was performed as we described in previous works.[37−40] Briefly, a chamber consisting of an 85 mm plastic Petri dish having a central hole in its bottom was glued to a plastic cylindrical vessel. Inside the chamber, polystyrene microbridges were filled with 35 μL of 200 mM $CaCl_2$ solution in 200 mM TRIS buffer. The cylindrical vessel contained 3 mL of 25 mM NH_4HCO_3 solution. All experiments were carried out inside the Petri dish using three different c-PANI polymers at different concentrations (32 and 64 μg/mL, and 1−1.6 mg/mL) at 20 °C for 24 h. Crystallization of $CaCO_3$ results from the diffusion of CO_2 vapor into the buffered $CaCl_2$ solution. The $CaCO_3$ crystals were rinsed with distilled water, dehydrated in a 50−100% gradient ethanol solution, dried at room temperature, and characterized. Additionally, $CaCO_3$ crystals were prepared by slow crystallization following the method of Kitano et al.[29−31] Briefly, a supersaturated solution of $CaCO_3$ was obtained by bubbling CO_2 gas through a solution of 5 g of $CaCO_3$ in 4 L of pure water for 60 min to shift the $CaCO_3$/$Ca(HCO_3)_2$ equilibrium toward the more water-soluble $Ca(HCO_3)_2$. The $CaCO_3$ was subsequently filtered off. Next, to dissolve the remaining $CaCO_3$ particles, CO_2 was bubbled through for another 30 min. A volume of 100 mL of Kitano solution and of c-PANI-1 polymer solution as an additive were left in a standard unsealed Petri dish (8.6 × 1.5 cm). For c-PANI-2 and c-PANI-3, only 20 mL was used and left in a small unsealed Petri dish (5.0 × 1.5 cm). For all crystallization reactions, the concentration of c-PANIs was 1 g/L. Carbon dioxide is formed on a time scale of hours to days, and the equilibrium shifts back to $CaCO_3$ under generation of a $CaCO_3$ supersaturation in the aqueous phase starting at the air−water interface. The Kitano method runs on a longer time scale as compared to the above-mentioned gas diffusion technique in order to exclude kinetic effects in the precipitation experiment. Crystals of $CaCO_3$ with well-defined morphology and reproducible size and surface area were normally found within 1 or 2 days. Typical rhombohedral crystals of calcite were obtained in the absence of additives, whereas c-PANIs additives yielded new $CaCO_3$ crystal morphologies.

2.5. Quantitative Calcium Titration and Crystallization. pH value and calcium measurements were performed using two 809 Titrando titration automats equipped with four 800 Dosino dosing devices, which operate a 2 mL 807 dosing unit (Metrohm). We utilized one pH electrode (Metrohm, no. 6.0227.100) and one Ca^{2+} ion selective electrode (Metrohm, no. 6.0508.110). The reference system of the pH electrode is gripped for calcium potential measurements.

(33) Salavagione, H. J.; Acevedo, D. F.; Miras, M. C.; Motheo, A. J.; Barbero, C. A. *J. Polym. Sci., Part A: Polym. Chem.* **2004**, *42*, 5587–5599.

(34) MacDiarmid, A. G., Chinag, J. C., Richter, A. F., Somarsiri, N. L. D., Epstein, A. J., Alacer, L., Eds. *Conducting Polymers*; Reidel Publishing Co.: Dordrecht, Holland, 1987; p 105.

(35) Cao, Y.; Andreatta, A.; Heeger, A. J.; Smith, P. *Polymer* **1989**, *30*, 2305–2306.

(36) Arias-Pardilla, J.; Salavagione, H. J.; Barbero, C.; Murallón, E.; Vázquez, J. L. *Eur. Polym. J.* **2006**, *42*, 1521–1532.

(37) Neira-Carrillo, A.; Yazdani-Pedram, M.; Retuert, J.; Diaz-Dosque, M.; Gallois, S.; Arias, J. L. *J. Colloid Interface Sci.* **2005**, *286*, 134–141.

(38) Arias, J. I.; Wiff, J. P.; Fernandez, M. S.; Fuenzalida, V.; Arias, J. L. *Mater. Res. Soc. Symp. Proc.* **2002**, *711*, 243–248.

(39) Neira-Carrillo, A.; Retuert, J.; Martinez, F.; Arias, J. L. *J. Chil. Chem. Soc.* **2008**, *53*, 1367–1372.

(40) Neira-Carrillo, A.; Pai, R. K.; Fuenzalida, V. M.; Fernández, M. S.; Retuert, J.; Arias, J. L. *J. Chil. Chem. Soc.* **2008**, *53*, 1469–1473.

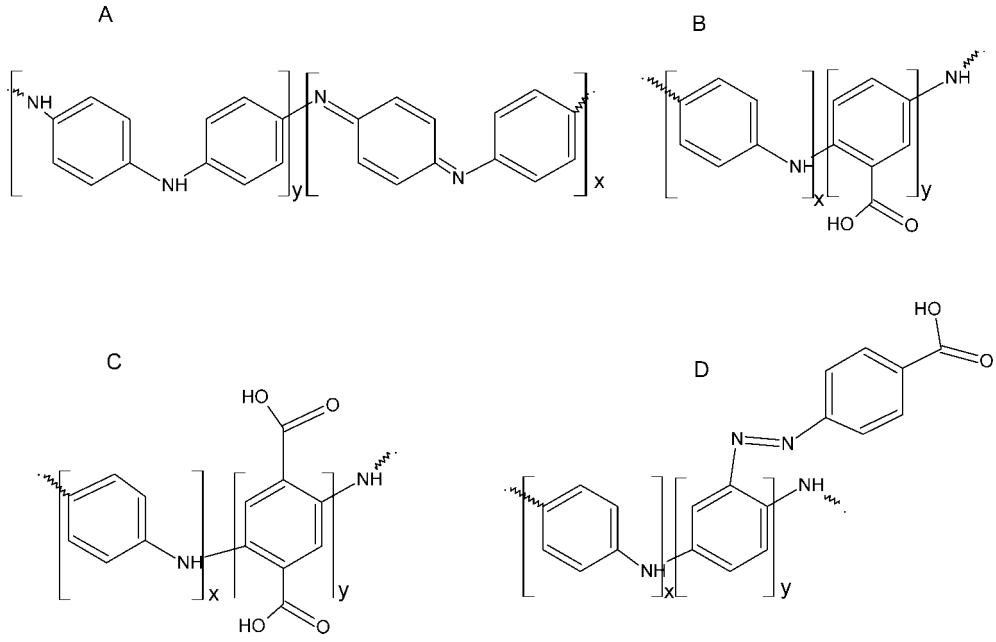

Figure 1. Chemical structures of the conducting polymers based on polyaniline: (A) polyaniline (PANI), (B) c-PANI-1, (C) c-PANI-2, and (D) c-PANI-3.

Calcium potential measurements are performed under N_2 atmosphere, which is provided by a nitrogen shower. The nitrogen shower is not utilized in crystallization experiments, because the removal of physically dissolved CO_2 from the carbonate buffer significantly reduces the total carbonate concentration. However, the N_2 atmosphere is crucial in calcium titration and calibration, because in-diffusion of atmospheric CO_2 produces an increasing carbonate concentration, which interferes with the measurements. N_2 gas is pipelined through a wash bottle filled with water in order to saturate the N_2 gas, and then directed onto the solution's surface, whereas the beaker is sealed against the air atmosphere using Parafilm in order to provide a minimum size outlet for the N_2 gas. The full experimental procedure for the calibration of electrodes is explained in the Supporting Information (section SI-1).

2.5.1. Crystallization Experiments. A 10 mM $CaCl_2$ solution (see above) was dosed at a rate of 20 μL/min into 25 mL of 9.4 mM carbonate buffer pH = 9.00 (prepared from a mixture of 10 mM sodium carbonate (Sigma, 99.95−100.05%, no. 223484) and 10 mM sodium bicarbonate (Acros Organics, ACS grade, no. 424270010) solutions giving the desired pH value). Here, the pH value was kept constant by titration with 10 mM NaOH (see above), because the pH value tends to decrease due to the precipitation of $CaCO_3$. The same experiments were performed with 25 mL of 9.4 mM carbonate buffer with 64 μg/mL PANI polymer (sedimenting suspension) and 64 μg/mL c-PANI-I (soluble).

2.5.2. Calcium Titration. Calcium titration was performed in analogy to the calibration of the Ca^{2+} ion sensitive electrode, whereas the 10 mM $CaCl_2$ solution was dosed into 25 mL of 1 mg/mL PANI (sedimenting suspension) and 1 mg/mL c-PANI-I (soluble) under N_2 atmosphere.

3. Results and Discussion

For the crystallization of $CaCO_3$ using the gas diffusion and Kitano methods, chemical structures of c-PANI polymers were used as illustrated in Figure 1.

We used three concentrations of c-PANI of 32 and 64 μg/mL and 1.0 mg/mL in gas diffusion experiments. It was found that both the concentration of c-PANI polymers and the presence of carboxylic acid groups on the PANI backbone have a strong influence on the crystallization behavior, polymorph occurrence, and morphology of the $CaCO_3$ crystals. Polymer concentration is crucial to control the $CaCO_3$ crystal morphology (Figure 2). At low concentration in the range of 32−64 μg/mL, c-PANI shows a transition of $CaCO_3$ rhombohedral to irregular shaped morphologies, which still express {104} faces. At 32 μg/mL, the morphology is still the standard calcite rhombohedra, and this concentration can be considered to be the lower polymer concentration limit for morphology control. Nevertheless, already at such low polymer concentrations, several rhombohedra are intergrown. With increasing c-PANI concentration, the morphology deviates from the default rhombohedra with six {104} faces and new faces become exposed. This indicates a face selective c-PANI adsorption. When the concentration is 1.0 mg/mL, c-PANI shows a strong and regular effect on the $CaCO_3$ morphology, whereas c-PANI-1 and c-PANI-2 with inflexible carboxy groups lead to crystals, in which remainders of the {104} faces can still be recognized as smooth faces. c-PANI-3 with flexible carboxy groups modifies the morphology completely (Figure 2C3), and the crystal appears to be polycrystalline. Generally, the $CaCO_3$ rhombohedra are intergrown in contrast to the reference experiment without c-PANI polymer. This effect is most pronounced for c-PANI-3, which has a flexible carboxylate group in contrast to PANI polymer.

For an even higher polymer concentration, Figure 3a shows control calcite crystals (rhombohedra) obtained in the presence of PANI without carboxylic acid groups attached to the polymer backbone. However, irregular $CaCO_3$ morphologies (Figure 3B−D) were grown if c-PANI presented carboxylic groups. Therefore, the presence of carboxylic groups along the c-PANI chain allows for interaction with $CaCO_3$ surfaces and thus the transition from a single crystal modified by face selective additive adsorption to a polycrystal. The Ca^{2+} ion binding capacity is illustrated for PANI and c-PANI-1 in Figure 4, proving that PANI (without carboxylic acid groups) does not exhibit Ca^{2+} ion binding capacity, whereas c-PANI-1 (with carboxylic acid groups) adsorbs Ca^{2+} ions until saturation of the polymer functional groups with a capacity of approximately 1% (m/m, based on monomer units), after which the detected Ca^{2+} concentration in solution rises linearly but still proportional to the amount of added Ca^{2+}. This loss of Ca^{2+} even under saturated solutions could very recently be attributed to the formation of

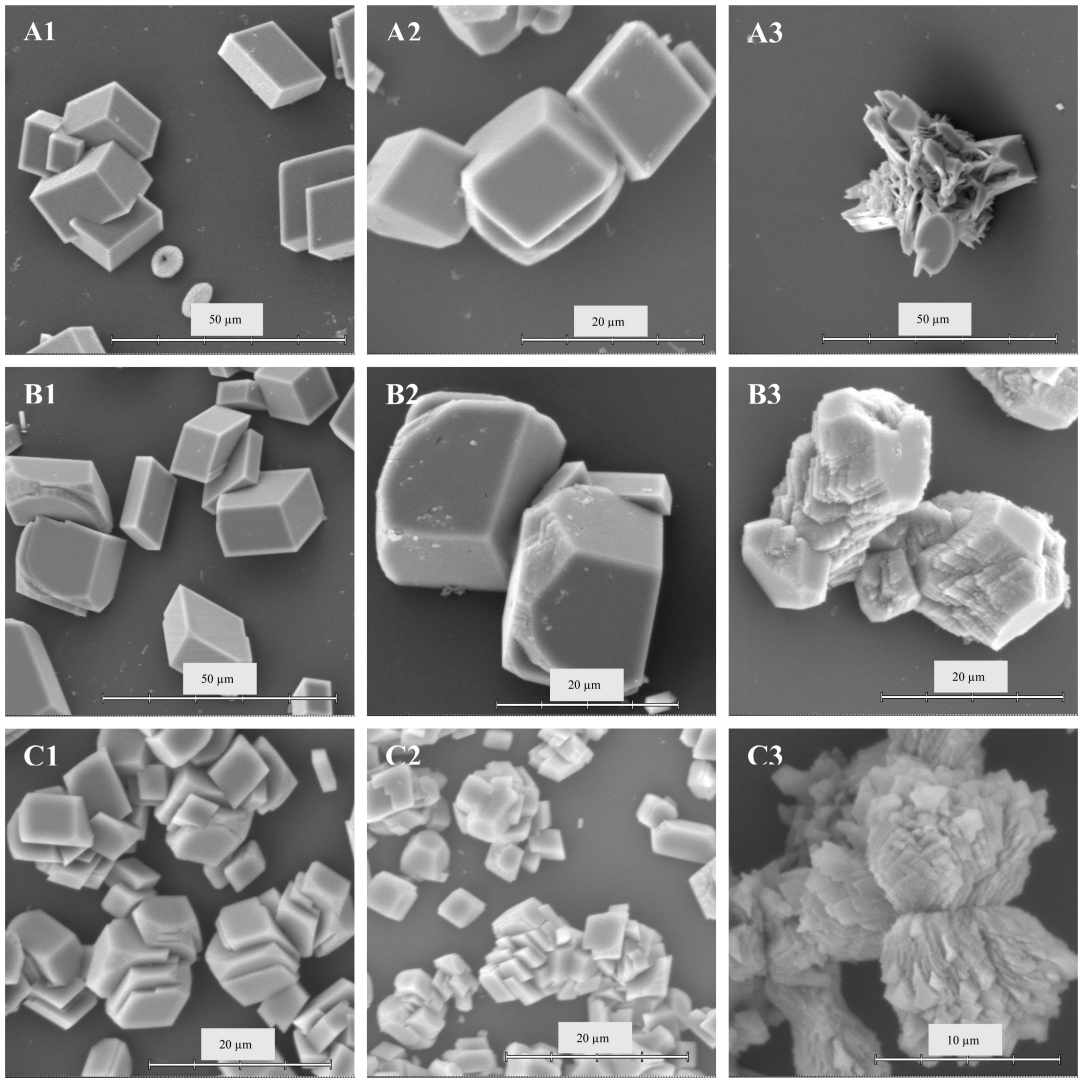

Figure 2. SEM images of $CaCO_3$ crystals grown at different concentrations using gas diffusion crystallization. (top) c-PANI-1: (A1) 32 μg/mL; (A2) 64 μg/mL; (A3) 1.0 mg/mL. (middle) c-PANI-2: (B1) 32 μg/mL; (B2) 64 μg/mL; (B3) 1.0 mg/mL. (bottom) c-PANI-3: (C1) 32 μg/mL; (C2) 64 μg/mL; (C3) 1.0 mg/mL.

subcritical $CaCO_3$ clusters.[41,42] When c-PANI-1 is used as the additive (Figure 3B), modified $CaCO_3$ crystals with three flat surfaces likely corresponding to the {104} faces are obtained. They also show irregular zones in between due to the polymer adsorption process. Figure 3C shows elongated intergrown calcite crystals for c-PANI-2 with orientational relationships, and rosette-like crystals without mutual orientation are obtained with c-PANI-3 (Figure 3D). The presence of a lateral and flexible carboxylic acid group along the c-PANI chain allows good adsorption onto crystal surfaces as indicated by Ca^{2+} binding capability illustrated in Figure 4 and finally leads to the aggregation of several primary particles to rosette-like crystals.

In order to determine the presence of c-PANI adsorbed on the crystal surface, energy dispersive X-ray spectroscopy (EDX) was used as a qualitative spatially resolved detection technique. Although a strong effect of c-PANI polymers on $CaCO_3$ morphology by SEM is obvious, probably the low concentration of the polymer and the small volume of total solution (35 μL) used during the gas diffusion method do not allow for the determination of the presence of nitrogen (atom %) adsorbed on the crystal surface (Figure 5). When applying c-PANI-1 as the additive, the EDX measurement shows the theoretical calcium/oxygen ratio (Ca/O = 1:3) only in the flat area ($\diamond$ in image) corresponding to pure calcite surfaces. However, when the irregular area (* in image) is analyzed, the ratio changes from Ca/O = 1:1.9, via 1:3.9, 1:4.30 to 1:6.1, which indicates the adsorbed polymer in largely varying amount on these faces (Figure 5A). For the modified crystal obtained with c-PANI-2, different ratios to the theoretical value are found; the ratio changes to C/O = 1:3.47, 1:3.56, and 1:5.47 (Figure 5B). For the rosette-like crystal obtained with c-PANI-3, always different ratios from the theoretical values of C/O = 1:2.60, 1:3.27, 1:3.47, and 1:4.17 are found (Figure 5C). This observation allows us to suggest that the adsorption of the c-PANIs occurs preferentially on the irregular surfaces and the rough surfaces are covered by c-PANI polymer. Different EDX measurement positions on the $CaCO_3$ crystals obtained with c-PANI additives, calculation of the C/O ratio, and the standards used for each atom are provided in the Supporting Information (Figure SI-2). These results are in qualitative agreement with the early observations of face selective adsorption of α,ω-dicarboxylic acids, which also revealed rough facets for the additive adsorption sites. [43] As the oxygen content

(41) Gebauer, D. Ph.D. Thesis, Potsdam University, 2008.
(42) Gebauer, D.; Cölfen, H. *Science*, submitted for publication.

(43) Mann, S.; Didymus, J. M.; Sanderson, N. P. *J. Chem. Soc., Faraday Trans.* **1990**, *86*, 1873–1880.

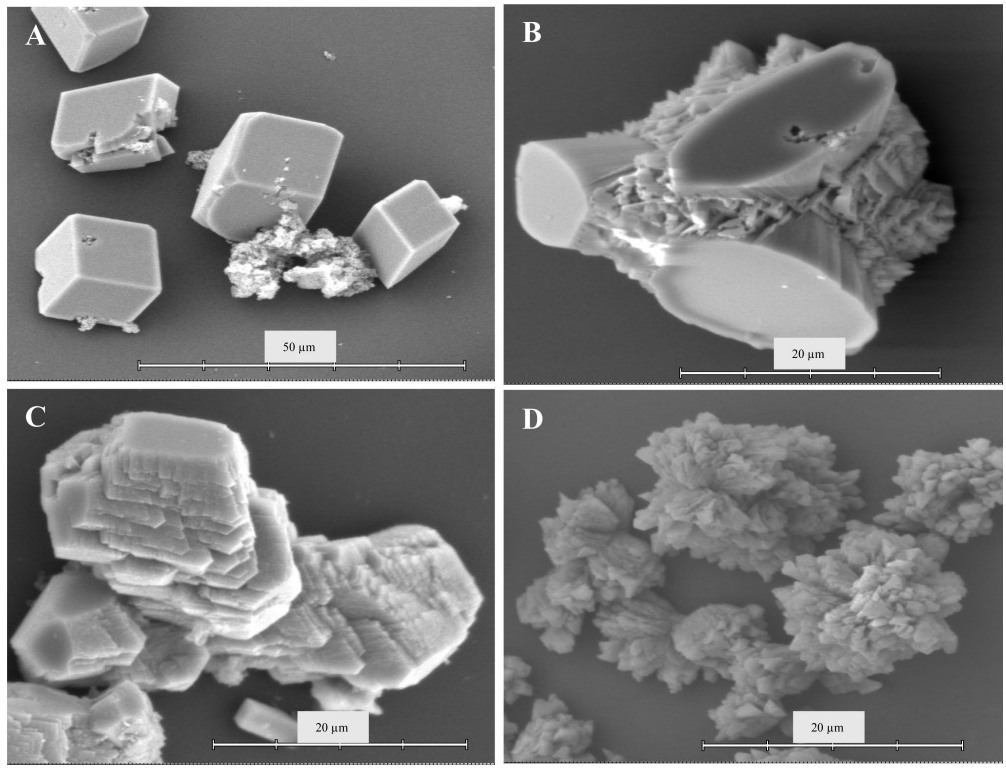

Figure 3. SEM images of $CaCO_3$ crystals grown using gas diffusion crystallization: (A) PANI, (B) c-PANI-1, (C) c-PANI-2, and (D) c-PANI-3. The concentration of the conducting polymers was 1.6 mg/mL.

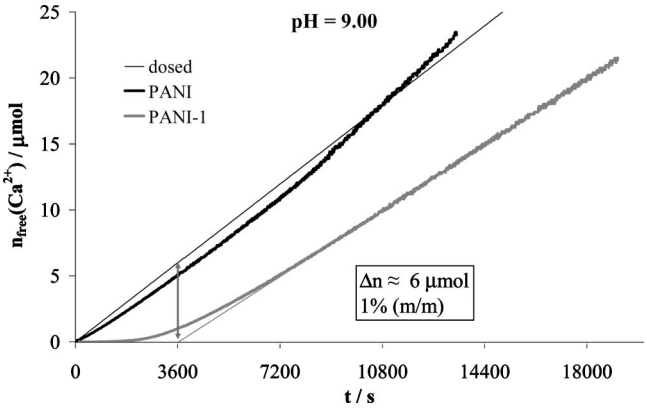

Figure 4. Calcium titration of PANI and c-PANI-1 at pH = 9.00 with polymer concentrations of 1 mg/mL. The time development of the dosed amount of Ca^{2+} ions gives the reference development. PANI does not exhibit Ca^{2+} ion adsorption. c-PANI-1 exhibits minor Ca^{2+} binding capacity according to approximately 1% (m/m).

is lower than the one expected for $CaCO_3$, the surfaces with adsorbed c-PANI get depleted of carbonate, indicative of electrostatic interaction between the polymer and surface exposed Ca^{2+} ions. This also agrees with the finding that c-PANI is not found on the neutral {104} faces. From the Ca/O ratio, the upper limit for the amount of adsorbed c-PANI polymer can be roughly estimated assuming that EDX only detected the surface composition and that each of the polymer carboxy groups adsorbs and depletes one carbonate ion. This means that, per adsorbed monomer unit of c-PANI-1 and c-PANI-3, one oxygen is missing if compared to pure $CaCO_3$. For c-PANI-2, two oxygens are missing in the balance per adsorbed monomer unit with two carboxy groups. For c-PANI-1, Ca/O is detected as 1:1.19, meaning that, for 100 Ca^{2+}, 11 oxygens are missing in the balance corresponding to 11 adsorbed monomer units.

The Kitano method allows us to study the effect of c-PANI as the additive in a slow crystallization process, in which the kinetic effects disappear. The Kitano experiment shows highly reproducible kinetics with a slow nucleation with defined and detectable nucleation and growth times (see Figure SI-3 in the Supporting Information). Here, the presence of carboxylic acid groups on the c-PANI backbone shows a similar influence on the $CaCO_3$ crystallization behavior and crystal morphology as discussed above for the gas diffusion method showing that the c-PANI influence on crystal morphology is prevailing kinetic differences in the applied crystallization methods. In order to learn more about the influence of the c-PANI polymers on the crystallization process, we measured the evolution of the amount of Ca^{2+} ions during $CaCO_3$ nucleation. Figure 6 shows the time development of the free amount of Ca^{2+} ions during slow addition of 10 mM $CaCl_2$ solution into 9.4 mM carbonate buffer at pH = constant = 9.0. The reference line indicates an experiment without any additives; PANI and c-PANI-1 indicate experiments with 64 μg/mL conducting polymer. The particular time developments are distinctly flatter than that of the dosed amount of Ca^{2+} ions. This can be attributed to the formation of prenucleation stage $CaCO_3$ clusters, because the Ca^{2+} ion sensitive electrode detects only hydrated ions. The solute clustering is described elsewhere in detail.[41,42] The discussed experiments are performed at pH = constant = 9.0, which is facilitated by pH = constant titration by means of 10 mM NaOH. The pH = constant titration facilitates the calculation of carbonate ions, which are bound in clusters and particles. The experiments show that carbonate and calcium binding are congruent. The particular prenucleation stage time developments are congruent within experimental accuracy; that is, the polymers have no distinct influence on prenucleation stage cluster formation, because an influence on cluster formation equilibria would be indicated by altered prenucleation stage slopes if compared to the reference experiment.[44] However, PANI promotes nucleation and c-PANI-1

inhibits nucleation of $CaCO_3$. We attribute the early nucleation of $CaCO_3$ in the presence of PANI to heterogeneous nucleation on insoluble polymer particles, because PANI is not completely soluble in carbonate buffer, giving a sedimenting particle suspension.

The inhibition of $CaCO_3$ nucleation in presence of c-PANI-1 can not simply be ascribed to the adsorption of Ca^{2+} ions on c-PANI-1 as illustrated in Figure 4, because the adsorption of Ca^{2+} ions is insignificant in the prenucleation stage as illustrated in Figure 6. In fact, the polymer stabilizes the prenucleation stage clusters against nucleation. Most likely, this is due to adsorption of the polymer onto subcritical clusters.

The carbonate buffer equilibrium may be written as

$$\{CO_{2,aq} + H_2O \leftrightarrow [H_2CO_{3,aq}]\} \overset{K_1}{\rightleftharpoons} H^+_{aq} + HCO^-_{3,aq} \overset{K_2}{\rightleftharpoons} 2H^+_{aq} + CO^{2-}_{3,aq} \quad (1)$$

while the concentration of carbonic acid is very low and $c([H_2CO_{3,aq}]) \cong c(CO_{2,aq})$.

The acid constants are given by $pK_1 = 6.35$ and $pK_2 = 10.33$.[45] Assuming physicochemical ideality, the law of mass action and the principle of mass preservation applied to eq 1 give for the concentrations of the three predominant species

$$c([CO_{2,aq}]) = c_{total}(\text{carbonate})\left[\frac{K_1}{c(H^+)} + \frac{K_1K_2}{c(H^+)^2} + 1\right]^{-1} \quad (2)$$

$$c(HCO^-_{3,aq}) = c_{total}(\text{carbonate})\left[\frac{c(H^+)}{K_1} + \frac{K_2}{c(H^+)} + 1\right]^{-1} \quad (3)$$

and

$$c(CO^{2-}_{3,aq}) = c_{total}(\text{carbonate})\left[\frac{c(H^+)^2}{K_1K_2} + \frac{c(H^+)}{K_2} + 1\right]^{-1} \quad (4)$$

From eqs 2 to 4, it is obvious that the carbonate buffer exhibits a constant ratio of the three species at constant pH values. The ratio of the three species at pH = constant = 9.00 is $CO_{2,aq}/HCO^-_{3,aq}/CO^{2-}_{3,aq} = 0.2{:}95.3{:}4.5$. Thus, formation of prenucleation

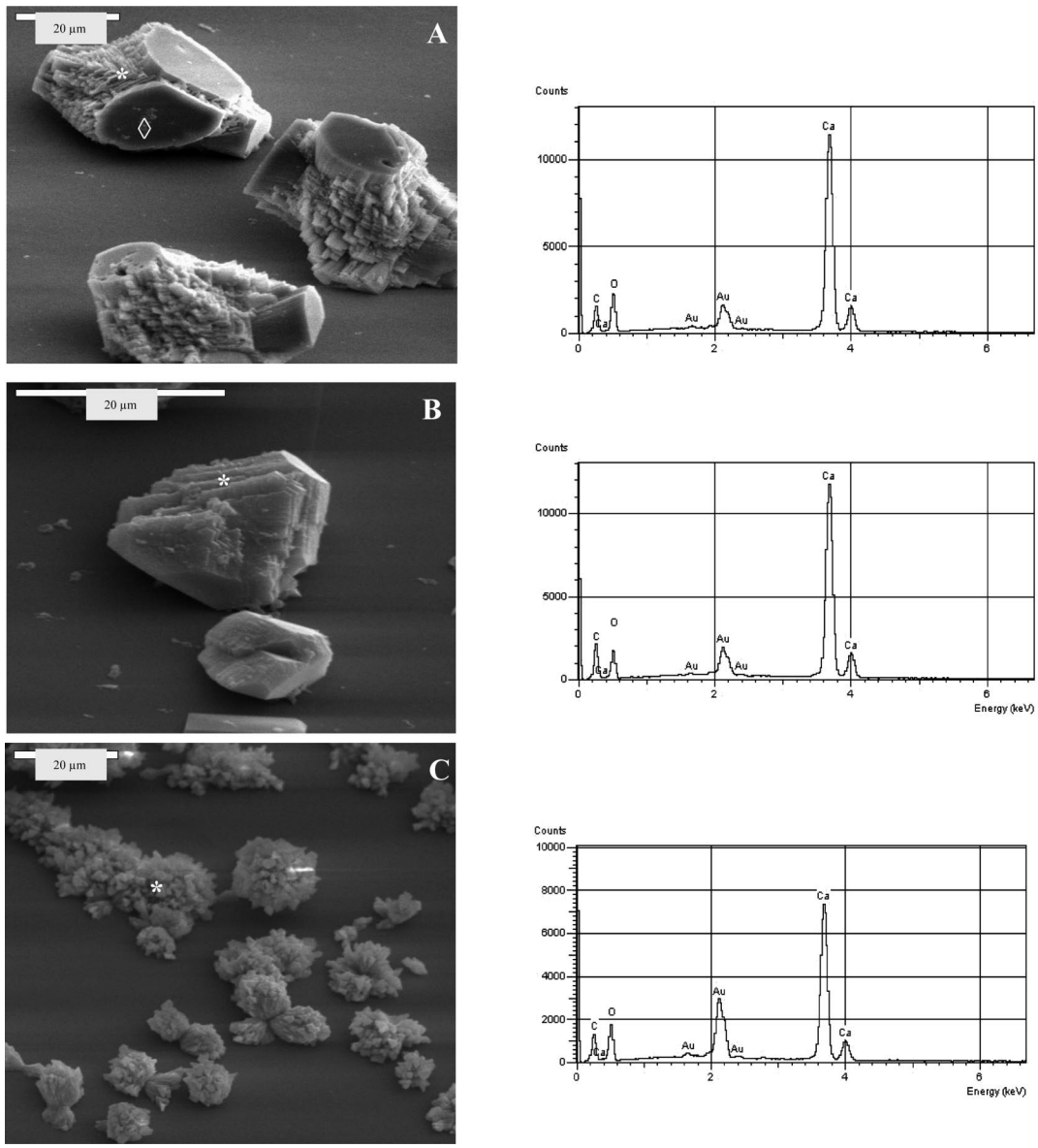

Figure 5. EDX spectra of $CaCO_3$ crystals obtained from conducting polymers using gas diffusion crystallization at 1.0 mg/mL: (A) c-PANI-1, (B) c-PANI-2, and (C) c-PANI-3. Nitrogen from the polymers is not detected due to a too low polymer amount.

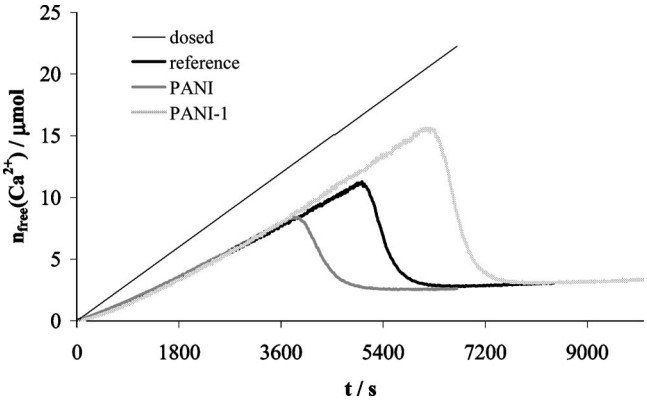

Figure 6. Time development of the free amount of Ca^{2+} ions due to slow addition of 10 mM calcium solution into 9.4 mM carbonate buffer at pH = constant = 9.0. The time development of the reference experiment (no additive) and the experiments with 64 μg/mL conducting polymer are distinctly flatter than that of the dosed amount of Ca^{2+} ions. This can be attributed to prenucleation stage $CaCO_3$ clusters. Within experimental accuracy, the prenucleation time developments are congruent, whereas PANI induces early nucleation and c-PANI-1 inhibits nucleation. For further explanations, see the text.

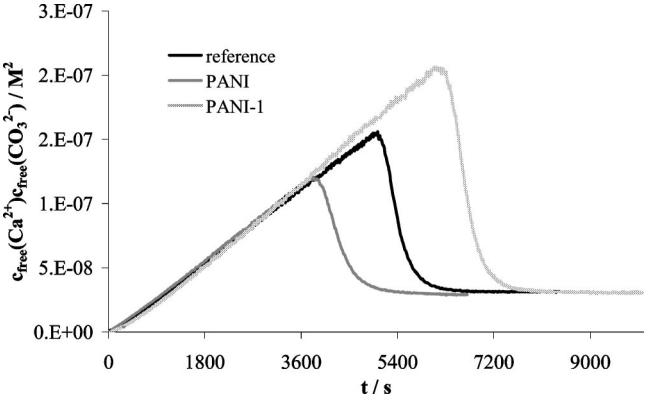

Figure 7. Time development of the free ion product. For further explanations, see the text.

stage $CaCO_3$ clusters, that is, the removal of carbonate ions from equilibrium (eq 1) generates protons. This can be simplified by Moreover, the binding of a carbonate ion in clusters corresponds

$$Ca^{2+}_{aq.} + HCO^{-}_{3,aq.} \rightleftharpoons (CaCO_3)_{cluster,aq.} + H^{+}_{aq.} \qquad (5)$$

to the removal of a diprotic base, which has to be exchanged by OH^- in order to keep the pH value constant. Thus, the time development of dilute NaOH necessary in pH = constant titration can be converted to the amount of carbonate ions bound in clusters. In this way, it can be shown that equal amounts of calcium and carbonate are bound in prenucleation stage clusters and in nucleated particles both in the absence of additives and in the presence of PANI and c-PANI-1 (data not shown). The knowledge of the particular bound and free amount of calcium and carbonate ions, respectively, facilitates the calculation of the time development of the ion product of free ions, which is illustrated in Figure 7. This curve is analogous to the classical LaMer nucleation curves.[46] Within experimental accuracy, the prenucleation stage time development of the ion product is congruent with and without polymer additive. After nucleation, the ion product declines rapidly and reaches the solubility product of amorphous calcium carbonate (ACC) of approximately 3.1×10^{-8} M².[41,42]

The time development of the ion product facilitates the calculation of the supersaturation S at the time of nucleation (TON),

$$S = \frac{[c_{free}(Ca^{2+}_{aq})c_{free}(CO^{2-}_{3,aq})]_{TON}}{[c_{free}(Ca^{2+}_{aq})c_{free}(CO^{2-}_{3,aq})]_{ACC}} \qquad (6)$$

We find $S \approx 5$ without additive, $S \approx 4$ in the presence of PANI, and $S \approx 6.5$ in the presence of c-PANI-1 at the point of nucleation. This further supports the nucleation promoting effect of PANI and the nucleation inhibition effect of c-PANI-1.

Figure 8 shows light microscopy images of $CaCO_3$ crystal formation using the PANI polymer as the additive. The pH evolution curve of PANI during $CaCO_3$ crystallization is shown in Figure SI-4 in the Supporting Information and compared with those of Kitano solution and c-PANI-1. Figure 8A shows only homogeneous spherical $CaCO_3$ particles before the maximum pH value of the solution is reached (50 min). After 60 min, shortly before the pH maximum is reached, a mixture of spherical particles and calcite rhombohedra is obtained (Figure 8B). Obviously, this corresponds to a transition stage of spherical ACC particles to calcite rhombohedra. Usually, such transitions occur via dissolution−recrystallization of the amorphous precursors, although extended X-ray absorption fine structure (EXAFS) studies on biogenic and synthetic ACC have shown local order in ACC which corresponds to the subsequent polymorph indicative of a solid state transformation.[47−50] Therefore, the exact transformation of ACC into calcite is not yet completely clarified. After this transition process, only calcite crystals are found (Figure 8C,D). However, Figure 8D shows smaller calcite particles than those in Figure 8C. This can be explained by the pH drop to pH 7.4. at 80 min; when this sample was taken, the pH value was still only 7.7. As the $CaCO_3$ solubility is pH-dependent, a pH drop increases the solubility and thus leads to partial dissolution of already existing calcite rhombohedra. Any remaining ACC material would have dissolved first upon the pH drop. Finally, when the pH value is rising again due to further evaporation of CO_2, the free Ca^{2+} ions precipitate with carbonate ions again and grow up to an equilibrium stage of calcite crystals controlled by the carbonate−bicarbonate buffer system. This time sequence clearly shows that the observation of the final crystal morphology does not necessarily provide the correct information about the crystallization process. Figure 9 shows three spherical $CaCO_3$ particles images obtained with c-PANI-1 at 40 min well before the maximum pH is reached at 220 min (cf. Figure 8A and Supporting Information Figure SI-4) using a digital microscope. The cross-polarization images of these particles demonstrate the amorphous character of the particles by the absence of birefringence. In addition, a large number of amorphous nanoparticles are present in solution, which are not visible by optical microscopy but can be revealed by TEM investigations (Figure 10). The electron diffraction (Figure 10, inset) of these spherical $CaCO_3$ particles shows an amorphous halo, proving the ACC character of the precursors for the final calcite particles.

(44) Gebauer, D.; Cölfen, H.; Verch, A.; Antonietti, M. *Adv. Mater.*, submitted for publication.
(45) Lide, D. R., Ed. *Handbook of Chemistry and Physics*, 75th ed.; CRC Press: Boca Raton, FL, 1994.
(46) LaMer, V. K.; Dinegar, R. H. *J. Am. Chem. Soc.* **1950**, *72*, 4847–4854.
(47) Addadi, L.; Raz, S.; Weiner, S. *Adv. Mater.* **2003**, *15*, 959–970.
(48) Lam, R. S. K.; Charnock, J. M.; Lennie, A.; Meldrum, F. C. *CrystEngComm* **2007**, *9*, 1226–1236.
(49) Politi, Y.; Levi-Kalisman, Y.; Raz, S.; Wilt, F.; Addadi, L.; Weiner, S.; Sagi, I. *Adv. Funct. Mater.* **2006**, *16*, 1289–1298.
(50) Hasse, B.; Ehrenberg, H.; Marxen, J. C.; Becker, W.; Epple, M. *Chem.−Eur. J.* **2000**, *6*, 3679–3685.

The above results clearly demonstrate that already particles are nucleated before the steep pH drop in the Kitano crystallization.

Figure 11A−D shows the SEM images of $CaCO_3$ crystals obtained after Kitano crystallization using 1.0 mg/mL c-PANI polymers for 48 h. Figure 11A shows again control calcite crystals (rhombohedra) with PANI without carboxylic groups attached on the backbone polymer. However, in contrast to the gas diffusion method, the {104} faces show pores, and the edges of the {104} rhombohedra are truncated. The pores in Figure 11A seem to follow a common grid of {104} faces, although they are not fully rhombohedral like those generated with templates after annealing.[51]

Moreover, irregular $CaCO_3$ morphologies (Figure 11B−D) are grown when c-PANI polymers bearing carboxylic groups are used. c-PANI-2 again causes an elongated calcite crystal morphology. For c-PANI-1 and c-PANI-3, the $CaCO_3$ crystal morphology is different. Rosette-like crystals are also obtained using c-PANI-1 (see Figure SI-5, Supporting Information). Although the effect of experimental variables on the polymorphs of $CaCO_3$ has been studied by many authors, the favorable conditions for obtaining each polymorph are generally uncertain. It is important to note that the gas diffusion method is likely to produce artifacts; the decomposition of NH_4HCO_3 velocity has been found to be strongly dependent on the utilized crystallization setup,[52] the dissolved ammonia can act as an additive,[53] and finally the pH is fixed by using TRIS buffer (pH = 9.0), which can also act as an additive. However, the advantage of the gas diffusion method is generally the small required sample volume, and therefore, it is often the only available method if little sample is available. The kinetic parameters are usually the determining factor of morphogenesis in the gas diffusion method. This is significantly different from the Kitano method, which gives the same basic effect of c-PANI, and thus, gas diffusion experiments present regular results.

Furthermore, X-ray diffraction of $CaCO_3$ particles obtained with Kitano experiments for all c-PANI polymers was performed. XRD analysis confirmed calcite as the stable polymorph (see Figure SI-6, Supporting Information) and showed calcite-like control crystals with only the {104} faces expressed when PANI was used. Although c-PANIs with carboxylic acid groups show also crystalline peaks corresponding to a calcite crystal, abundant other reflections as indicated in Figure SI-6B−D in the Supporting Information were found. c-PANI-1 shows an oriented calcite

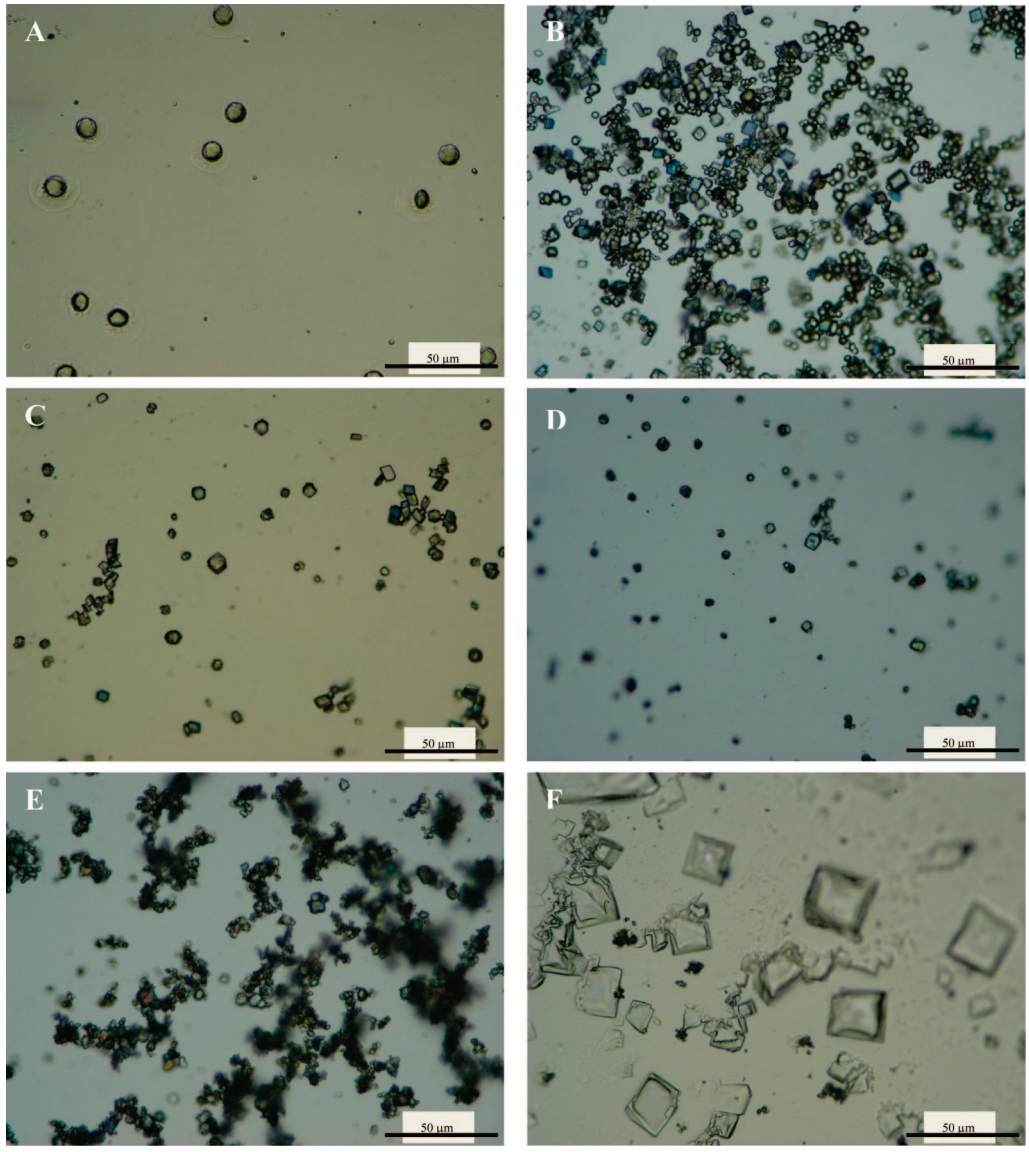

Figure 8. Light microscopy images showing in real time the formation of $CaCO_3$ particles using PANI by the Kitano method during pH measurements: (A) 40 min, (B) 60 min, (C) 80 min, (D) 100 min, (E) 7 h, and (F) 24 h.

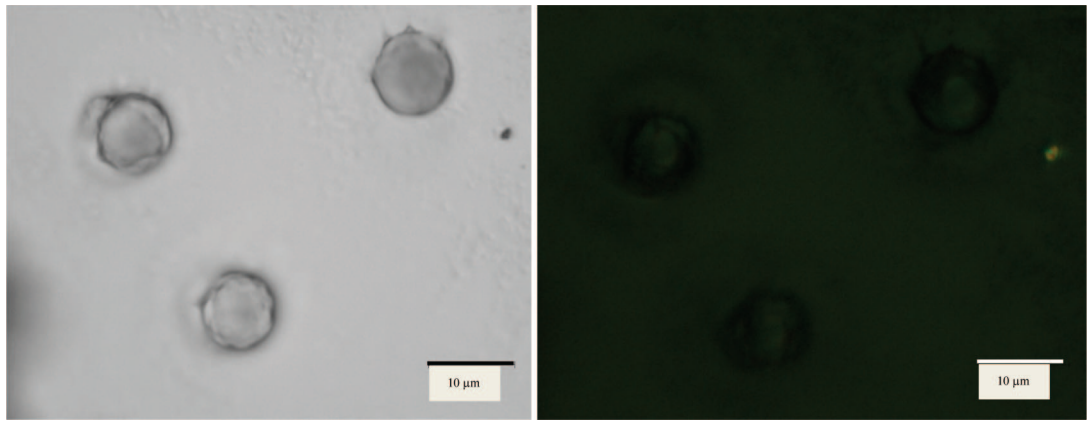

Figure 9. Spherical $CaCO_3$ crystals using c-PANI-1 obtained at 40 min: (left) digital images of $CaCO_3$ particles and (right) cross polarization image of $CaCO_3$ particles.

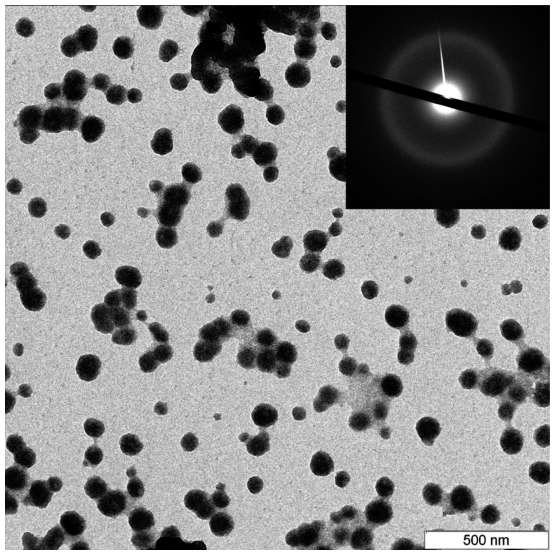

Figure 10. TEM micrograph of spherical $CaCO_3$ particles grown at 40 min. Inset corresponds to the electron diffraction pattern.

crystal with {110} faces as the principal family. For c-PANI-3, slightly broader reflections were found indicative of a lower coherence length. This qualitative observation is in agreement with the more pronounced interaction of the crystal with flexible carboxy groups, which is supported by the morphology modification observed by SEM (see Figure 2C3). All standard peak designations were obtained from the data file PCDDFWIN. The WAXS measurements obtained with the c-PANI polymers, in which calcite is nucleated, can also be confirmed by the absorption bands of calcite at 710 and 868 cm^{-1} using infrared spectroscopy (FTIR).[54,55] The specific absorption of the stretching vibration of quinonimine and aromatic rings of c-PANI can be easily recognized in the resulting $CaCO_3$ crystals[17] (see Figure SI-7 in the Supporting Information). In addition, a good assignment of the infrared vibration for c-PANI-1 with a different feed ratio of aniline is reported. In order to visualize the fluorescence induced by included c-PANI in $CaCO_3$ particles, we deposited homogeneously $CaCO_3$ crystals obtained from c-PANI-1 after Kitano crystallization on a glass substrate and observed them under a Nikon Eclipse E600 fluorescence microscope adapted with a CoolSNAP-Pro Color camera. The Image-pro Plus program was used for all fluorescence digital images (see Figure SI-8 in the Supporting Information). Tuning of the focus of the microscope reveals the fluorescence also from inside of the crystals (data not shown). We find that the fluorescence of $CaCO_3$ crystals using, for example, c-PANI-1 does not disappear after washing and drying processes of the $CaCO_3$ crystals, confirming that c-PANI-1 molecules are incorporated into the bulk of these crystals, similar to the case of fluorescent dyes as recently reported by Aizenberg and Han.[56] The present data strongly suggest the ability of c-PANI molecules to be incorporated into the crystal matrix in addition to the morphological modification of calcite. This observation allows for the understanding of the ability of c-PANI to change the energy landscape during the crystallization process and allows for interesting future materials applications.

4. Conclusion

In summary, conducting polymers offer a great range for polymer controlled crystallization applications. We used rigid c-PANI polymers having carboxylic acid groups attached to the PANI backbone to control $CaCO_3$ crystallization using gas diffusion and Kitano methods. It was found that different c-PANIs interacted differently with the individual growth planes of $CaCO_3$ crystals. It seems that the structural placement of the carboxy group in the polymer is determinant of its influence on the crystallization. Also, for the control of the nucleation and growth process, $CaCO_3$ varied significantly between c-PANIs. The gas diffusion method showed that the polymer concentration is crucial to control the $CaCO_3$ crystal morphology. At lower concentration of c-PANI, a transition of $CaCO_3$ crystals appears from rhombohedral to irregular shaped crystals. In addition, the crystals are intergrown for all c-PANI polymers. However, at higher concentration (ca. 1.0 mg/mL), the $CaCO_3$ crystal morphology is completely modified and great differences become obvious between the different polymers. PANI without carboxylic groups nucleates calcite but shows no effect on $CaCO_3$ crystals, and rhombohedral calcite crystals are always grown in both crystallization methods. Therefore, the presence of carboxylic groups along the c-PANI chain is crucial for interaction with the growing $CaCO_3$ as can be expected from numerous literature reports.[3,57−60]

(51) Page, M. G.; Nassif, N.; Börner, H.; Antonietti, M.; Cölfen, H. *Cryst. Growth Des.* **2008**, *8*, 1792–1794.
(52) Neira-Carrillo, A.; Fernández, M. S.; Retuert, J.; Arias, J. L. *Mater. Res. Soc. Proc.* **2003**, *EXS-1, H1*, 321–326.
(53) Gehrke, N.; Cölfen, H.; Pinna, N.; Antonietti, M.; Nassif, N. *Cryst. Growth Des.* **2005**, *5*, 1317–1379.
(54) Hosoda, N.; Kato, T. *Chem. Mater.* **2001**, *13*, 688–693.
(55) Gehrke, N.; Nassif, N.; Pinna, N.; Antonietti, M.; Gupta, H. S.; Cölfen, H. *Chem. Mater.* **2005**, *17*, 6514–6516.
(56) Han, T. Y-J.; Aizenberg, J. *Chem. Mater.* **2008**, *20*, 1064–1068.
(57) Rieger, J.; Thieme, J.; Schmidt, C. *Langmuir* **2000**, *16*, 8300–8305.
(58) Sedlak, M.; Cölfen, H. *Macromol. Chem. Phys.* **2001**, *202*, 587–597.

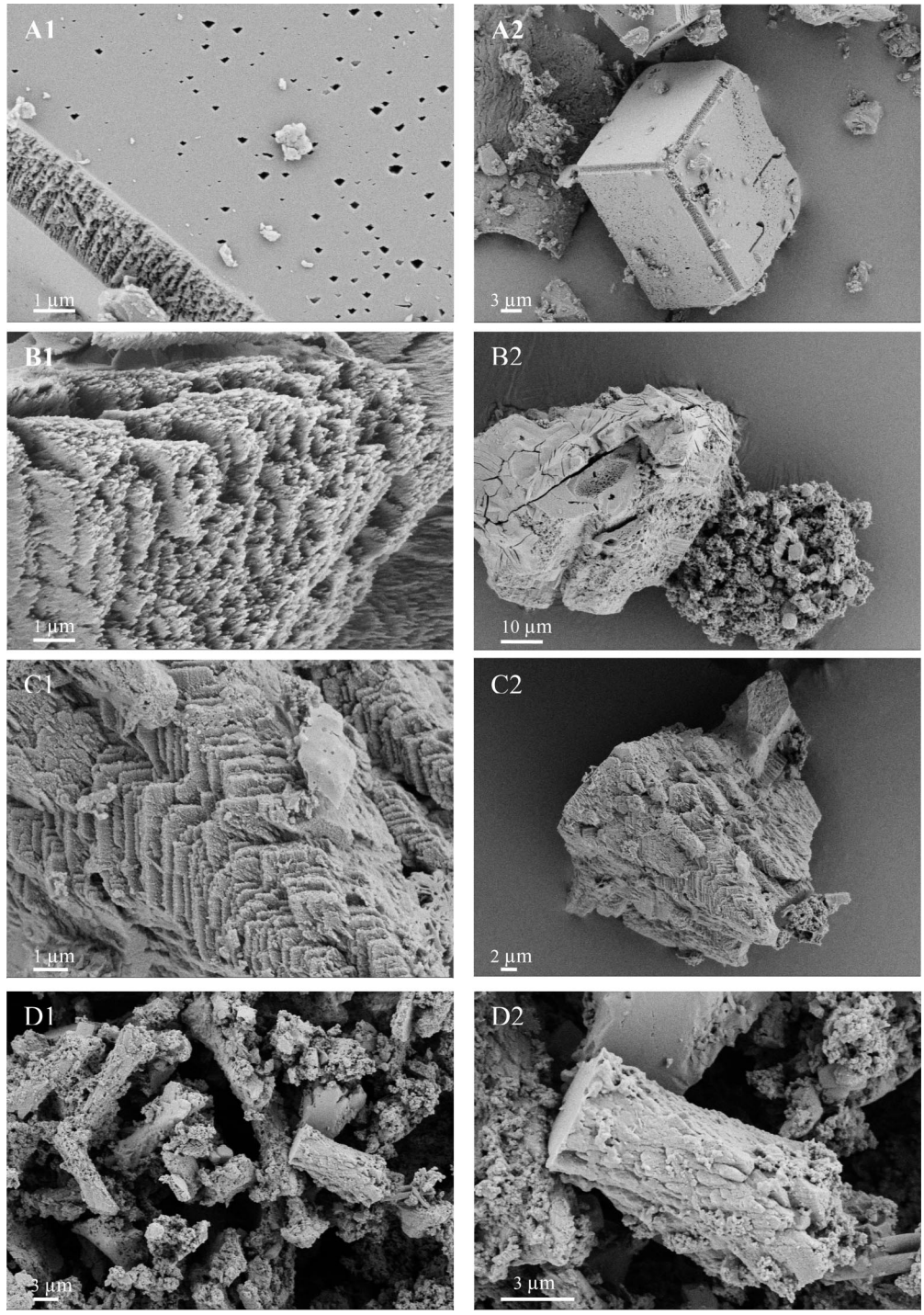

Figure 11. SEM images of CaCO3 crystals grown using the Kitano method at 1 mg/mL: (A) PANI, (B) c-PANI-1, (C) c-PANI-2, and (D) c-PANI-3. The concentration of the c-PANI polymers was 1.0 mg/mL.

By using the Kitano method, it is also possible to obtain small calcite particles and detect spherical ACC precursor particles corresponding to the first steps of crystallization. The Kitano method allowed us to study the effect of c-PANI as an additive in a slow crystallization process, in which the kinetic effects disappear. Time-dependent Ca^{2+} measurements reveal that PANI is a nucleation promoter whereas c-PANI polymers are crystallization inhibitors. The pH measurement in Kitano crystallization illustrates that the nucleation of $CaCO_3$ particles occurs in a defined time interval, and combination with light microscopy shows the transformation from spherical amorphous ACC particles to calcite crystals. A constant-pH approach can be used as a simple way to determine the effective reactant concentrations for mineralization for a wide concentration range of known synthetic polymers and biopolymers. XRD and FTIR revealed the calcite polymorph in all cases. The interesting feature of c-PANI controlled crystallization of calcite is the inclusion of the fluorescent polymer into the crystal lattice. This not only confirms earlier reports about intracrystalline biopolymers in

(59) Euliss, L. E.; Bartl, M. H.; Stucky, G. D. *J. Cryst. Growth* **2006**, *286*, 424–430.
(60) Gorna, K.; Muños-Espí, R.; Gröhn, F.; Wegner, G. *Macromol. Biosci.* **2007**, *7*, 163–173.

biominerals[61−63] but furthermore offers the design of interesting hybrid materials combining the biocompatibility of calcite with the fluorescence and conducting properties of the PANI polymers.

Acknowledgment. This research was supported by FONDAP 11980002 and FONDECYT 11070136 granted by the Chilean Council for Science and Technology (CONICYT). A.N.-C. thanks Prof. Markus Antonietti (MPI of Colloids and Interfaces, Golm, 14424, D-Potsdam, Germany) for the fruitful discussions. Ingrid Zenke is acknowledged for XRD, Rona Pitschke for SEM, and Irina Shekova and Jürgen Hartmann for SEM-EDX.

Supporting Information Available: Procedure for calibration of the electrodes; EDX measurements, pH evolution curves, SEM images, WAXS plots, FTIR spectra, and fluorescent light micrographs of $CaCO_3$ crystals. This material is available free of charge via the Internet at http://pubs.acs.org.

(61) Berman, A.; Addadi, L.; Weiner, S. *Nature* **1998**, *331*, 546–548.
(62) Addadi, L.; Weiner, S. *Proc. Natl. Acad. Sci. U.S.A.* **1985**, *82*, 4110–4114.
(63) Pokroy, B.; Fith, A. N.; Marin, F.; Kapon, M.; Adir, N.; Zolotoyabko, E. *J. Struct. Biol.* **2006**, *155*, 96–103.